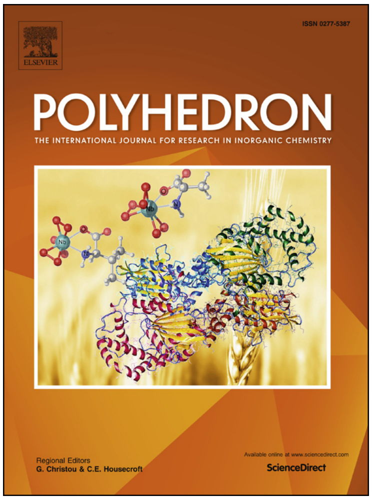

Synthesis and characterization of a ruthenium complex with bis(diphenylphosphino)propane and thioether containing ONS donor ligand: Application in transfer hydrogenation of ketones

Sujan Biswas, Deblina Sarkar, Puspendu Roy, Tapan Kumar Mondal

PII: S0277-5387(17)30288-7
DOI: http://dx.doi.org/10.1016/j.poly.2017.04.019
Reference: POLY 12597

To appear in: *Polyhedron*

Received Date: 2 February 2017
Revised Date: 11 April 2017
Accepted Date: 18 April 2017

Please cite this article as: S. Biswas, D. Sarkar, P. Roy, T. Kumar Mondal, Synthesis and characterization of a ruthenium complex with bis(diphenylphosphino)propane and thioether containing ONS donor ligand: Application in transfer hydrogenation of ketones, *Polyhedron* (2017), doi: http://dx.doi.org/10.1016/j.poly.2017.04.019

Synthesis and characterization of a ruthenium complex with bis(diphenylphosphino)propane and thioether containing ONS donor ligand: Application in transfer hydrogenation of ketones

Sujan Biswas, Deblina Sarkar, Puspendu Roy and Tapan Kumar Mondal*

Inorganic Chemistry Section, Department of Chemistry, Jadavpur University, Kolkata-700032, India.

Abstract

The synthesis and characterization of a mixed ligand Ru(II) complex, [Ru(dppp)(L)Cl] (**1**) (where, dppp = bis(diphenylphosphino) propane) is reported. The distorted octahedral geometry of the complex is confirmed by X-ray diffraction method. Cyclic voltammogram in CH_3CN exhibits Ru(II)/Ru(III) quasireversible oxidation couple along with reversible azo-bond reductions peaks with reference to Ag/AgCl electrode. The efficiency of the complex towards the transfer hydrogenation of ketones in *i*-PrOH is examined and an excellent catalytic conversion (90-98%) is observed. The electronic structure and redox properties are well corroborated with the DFT calculations.

Key words: Ruthenium complex; Thioether ligand; X-ray structure; Electrochemistry; Transfer hydrogenation of ketones; DFT calculation.

Corresponding author: Ph.: 91-033-24572970; Email: tkmondal@chemistry.jdvu.ac.in

1. Introduction

Transition metal complexes with phosphine ligands have important industrial applications because of their efficient catalytic activities [1, 2]. The electron donating and accepting ability of bis(dialkylphosphino)alkane ligands in metal complexes can be easily tuned with the variation of alkyl groups bonded to the phosphorus atoms [1, 3-5]. Moreover, this change affects the activity, basicity, selectivity and stability of catalytic processes [6, 7]. Tolman made a useful comparison between the electronic and the steric effects of these ligands [3].

Transfer hydrogenation of ketones to corresponding alcohols is one of the most important fundamental subjects in modern synthetic chemistry [8, 9] and is a convenient method to reduce carbonyl compounds without the use of hazardous hydrogen gas or moisture-sensitive hydride reagents [10-13]. Moreover, the transfer hydrogenation of ketones is widely accepted in industry as a cost-effective way for the production of a number of hydroxylated organic products [14]. The studies to develop the new catalysts for the transfer hydrogenation is still of considerable interest for the finding of more efficient catalyst. The most efficient and selective catalyst for transfer hydrogenation reactions are ruthenium, iridium and rhodium complexes [15-19]. The ‘‘Ru(P–P)” core is recognized as an active catalytic species for the hydrogenation of unsaturated carbonyl compounds [20-22]. Recently, mixed-ligand diamine-bis(diphosphine) ruthenium(II) complexes have received much attention due to their remarkable performance in selective and asymmetric hydrogenation of carbonyl compounds [23-26].

Azo group shows donor properties and play an important role in coordination chemistry [27-29]. Synthesis of ruthenium complexes with azo ligands and their usages in transfer hydrogenation, oxidation of alcohols and metal-carbon bond formation reactions are widely studied [29-31]. The ruthenium complexes with polydentate ligands also have significant importance in catalytic reactions [32-34]. As a part of our ongoing research on synthesis, characterization and catalytic applications of ruthenium complexes [35-38], in the present work we have synthesized a ruthenium(II) complex, [Ru(dppp)(L)Cl] (**1**) bearing bis(diphenylphosphino)propane (dppp) with ONS donor azo-thioether ligand, 3-(2-(2-(methylthio)phenyl)hydrazono)pentane-2,4-dione (HL) (scheme 1). An array of tools including X-ray diffractometry, electrochemistry, and electronic absorption and emission spectroscopy abetted with DFT calculations were used to characterize the complex. Further, the catalytic activity of the complex towards transfer hydrogenation of ketones was investigated.

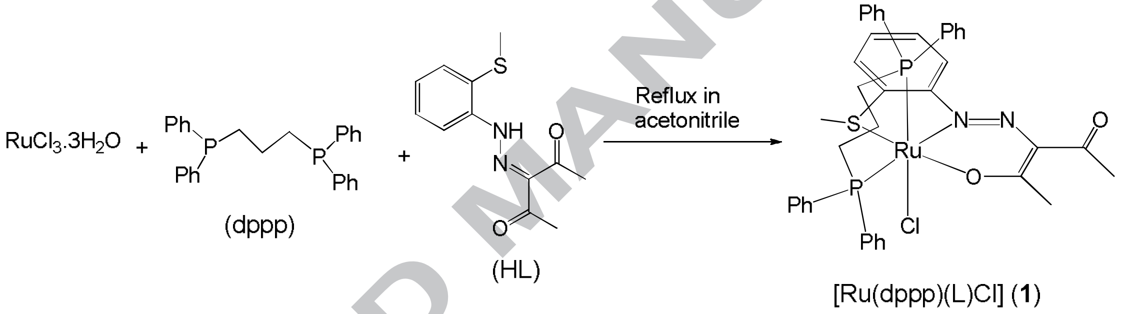

Scheme 1. Synthesis of ruthenium(II) complex, [Ru(dppp)(L)Cl] (**1**)

2. Experimental

2.1. Materials and methods

All the reagents and solvents were purchased from commercial sources and used as received. Acetylacetone and inorganic metal salts were obtained from E. Merck, India. 2-Aminothiophenol was purchased from Sigma Aldrich. 3-(2-(2-(Methylthio)phenyl)hydrazono)pentane-2,4-dione (HL) was prepared by following the published procedure [39]. Microanalyses (C, H, N) data were obtained using a PerkinElmer Series-II CHN-2400 CHNS/O elemental analyzer. Electronic spectra were measured on a Lambda 750 PerkinElmer spectrophotometer in acetonitrile. IR spectra were recorded on a RX-1 PerkinElmer spectrometer in the range of 4000-400 cm^{-1} with the samples in the form of KBr pellets. HRMS mass spectra were obtained on a Waters (Xevo G2 Q-TOF) mass spectrometer. NMR spectra were recorded in $CDCl_3$ on a Bruker (AC) 300 MHz FT-NMR spectrometer in the presence of TMS as internal standard. Cyclic voltammetric measurements were carried out using a CHI Electrochemical workstation. A platinum wire working electrode, a platinum wire auxiliary electrode and Ag/AgCl reference electrode were used in a standard three-electrode configuration. Bu_4NPF_6 was used as the supporting electrolyte in acetonitrile and the scan rate used was 50 mV s^{-1} under nitrogen atmosphere.

2.2. Synthesis of ruthenium(II) complex, [Ru(dppp)(L)Cl] (1)

$RuCl_3.3H_2O$ (0.13 g, 0.5 mmol) and 3-(2-(2-(methylthio)phenyl)hydrazono)pentane-2,4-dione (HL) (0.13 g, 0.5 mmol) were dissolved in 25 mL acetonitrile and refluxed for 1 h. After that bis(diphenylphosphino)propane (dppp) (0.20 g, 0.5 mmol) was added to the solution. The reaction mixture was heated for an additional 5 h. The solvent was then removed under reduced pressure. The crude product was dissolved in dichloromethane and purified by column chromatography using a silica gel (mesh 60-120). The orange band of **1** was eluted by 50% (v/v) ethyl acetate-petroleum ether mixture. On removal of the solvent under reduced pressure the pure complex **1** was obtained as an orange solid which was further dried under vacuum. Yield, 0.27 g (68%).

Anal. Calc. for $C_{39}H_{39}ClN_2O_2RuS$ (**1**): C, 58.68; H, 4.92; N, 3.51; S, 4.02%. Found: C, 58.26; H, 4.78; N, 3.42; S, 3.92%. IR data (KBr, cm^{-1}): 1665 υ(C=O); 1369 υ(N=N). ^{1}H NMR data ($CDCl_3$, ppm): 6.82-7.86 (24H, m, aromatic protons), 3.06 (4H, br, PCH_2), 2.67 (3H, s, SCH_3), 2.61 (2H, br, P CH_2CH_2), 2.52 (3H, s, CH_3), 2.39 (3H, s, CH_3). HRMS *m/z*, 821.3632

(M-Na$^+$: 821.26). $E_{1/2}$ (Ru^{II}/Ru^{III}): 1.12 V (ΔE = 95 mV); $E_{1/2}$(L/L$^{\bullet-}$): -0.89 V (ΔE = 75 mV) and E_{pc} (L$^{\bullet-}$/L^{2-}): -1.75 V.

2.3. Crystal structure determination and refinement

Single crystals of **1** were obtained by slow diffusion of *n*-hexane into dichloromethane solution of the complex. The crystal evaluation and data collection were performed on an automated Bruker AXS Kappa smart Apex-II diffractometer equipped with an Apex-II CCD area detector using a fine focus sealed tube as the radiation source of graphite monochromated Mo Kα radiation (λ = 0.71073 Å). The reflections were successfully indexed by an automated indexing routinebuilt into the APEX II programme suite [40]. Reflection data were recorded using the ω scan technique. The structure was solved and refined by full-matrix least-squares techniques on F^2 using the SHELX-97 [41]. The absorption corrections were done by multi-scan method and all the data were corrected for Lorentz, polarization effect. Hydrogen atoms were included in the refinement process as per the riding model. Details of crystal analyses, data collection and structure refinement are summarized in Table 1.

2.4. Computational method

Full geometry optimization of the complex was carried out by density functional theory (DFT) method using B3LYP hybrid exchange correlation functional [42,43]. All elements except ruthenium were assigned the 6-31G(d) basis set, whilst the LanL2DZ basis set with effective core potential was employed for ruthenium atom [44-46]. Vibrational frequency calculation was performed to ensure that the optimized geometry was in local minima on the potential energy surface and only positive Eigen values were obtained. Vertical electronic excitations based on B3LYP optimized geometry were computed using the time-dependent density functional theory (TDDFT) formalism [47-49] using conductor-like polarizable continuum model (CPCM) [50-52] in acetonitrile to simulate the solvent. All calculations were performed with Gaussian09 program package [53]. GaussSum [54] was used to calculate the fractional contributions of various groups to each molecular orbital.

2.5. Procedure of transfer hydrogenation of ketones

In a typical experiment the ketone (1 mmol), KOH (0.1 mmol), and ruthenium(II) complex (0.0025 mmol) were added to 10 mL of *i*-PrOH, and the mixture was stirred at 80 °C in an inert atmosphere. The reaction was then monitored at various time intervals by the use of GC. After the reaction was complete, *i*-PrOH was removed on a rotary evaporator, and the resulting semisolid was extracted with diethyl ether (5 × 10 mL). The extract was passed through a short column of silica gel. The column was washed with ~100 mL of diethyl ether. All the eluates from the column were mixed, and the solvent from the mixture was evaporated off on a rotary evaporator. The resulting residue was dissolved in 2-3 mL of hexane. Conversions were determined by GC instrument equipped with a flame ionization detector (FID) using a HP-5 column of 30 m length, 0.53 mm diameter and 5.00 μm film thickness. The column, injector and detector temperatures were 200, 250 and 250^0C respectively. The carrier gas was N_2 (UHP grade) at a flow rate of 30 mL/min. The injection volume of sample was 2 μL. The alcohols were identified by GC co-injection with authentic samples.

3. Results and discussion

3.1. Synthesis and formulation

The ligand, 3-(2-(2-(methylthio)phenyl)hydrazono)pentane-2,4-dione (HL) was prepared by following the published procedure [39]. The ruthenium(II) complex, [Ru(dppp)(L)Cl] (**1**) (where, dppp = bis(diphenylphosphino)propane) was synthesized by the reaction of $RuCl_3.3H_2O$, dppp and HL under refluxing condition in acetonitrile (scheme 1). The complex was characterized by various spectroscopic techniques. Mass spectrum and elemental analysis data support the composition of the complex (see experimental section). In the IR spectrum the bands at 1665 and 1369 cm^{-1} correspond to υ(C=O) and υ(N=N) respectively. The υ(N=N) appeared at lower frequency region compare to free ligand value supporting the coordination of azo-N to ruthenium(II) and extensive $d\pi(Ru) \rightarrow \pi^{*}(N=N)$ back donation in the complex. ^{1}H NMR spectrum of the complex was taken in $CDCl_3$. The aromatic proton signals appeared at 6.82-7.86 ppm region, while the expected singlet peaks correspond to S-CH_3 and CH_3 protons appeared at 2.67, 2.52 and 2.39 ppm. The P-CH_2 signals appeared as broad peaks at 3.06 and 2.61 ppm in the complex. The geometry of the complex was further confirmed by single crystal X-ray structure analysis.

3.2. X-ray structure of [Ru(dppp)(L)Cl] (1)

Single crystals suitable for structure determination were obtained by slow diffusion of n-hexane into dichloromethane solution of the complex. The crystallographic data collection and refinement parameters are given in Table 1; selected bond lengths and angles are given in Table 2. ORTEP plot with atomic numbering scheme is shown in Fig. 1. The ruthenium atom adopts a distorted octahedral geometry in the complex, as evidenced by P1-Ru1-P1 (92.00(4)º), O1-Ru1-N2 (87.62(11)º) and S1-Ru1-N2 (84.33(9)º) bite angles. The thioether ligand binds to the ruthenium atom by thioether-S, azo-N and O atom of acetyl acetonato moiety. The dppp ligand binds via its two P-atoms *trans* to the azo-N and Cl atoms, with Ru1-P1 and Ru1-P2 bond distances of 2.2802(11) and 2.3602(11) Å respectively. The Ru1-Cl1 (2.4680(10) Å), Ru1-N2 (2.044(3) Å) and Ru1-S1 (2.3031(10) Å) are in the typical range reported in the literature [55-57].

3.3. DFT computation and electronic structure

The geometry of complex **1** was optimized by DFT method in singlet ground state using the B3LYP correlation functional. The optimized bond parameters are given in Table 2. The calculated bond distances and angles are well correlated with the X-ray crystal structure data.

The contour plots of selected molecular orbitals of the complex are shown in Fig. 2, while the energy and compositions are summarized in Table 3. The HOMO to HOMO-3 are composed of mixed $d\pi$(Ru) (29-47%) and π(L) (21-50%) orbitals along with significant contribution of $p\pi$(Cl) (10-39%) orbitals. The LUMO has π^*(L) character (94%) with major contribution of π^*(N=N) orbital (42%) and the HOMO-LUMO energy gap in the complex is 3.45 eV. LUMO+1 to LUMO+5 are composed of π^*(dppp) orbitals along with reduced contribution of $d\pi$(Ru) and π^*(L).

3.4. TDDFT calculation and electronic spectra

The solution spectrum of complex **1** in acetonitrile exhibits moderately intense broad peak at 466 nm (ε = 3907 M^{-1} cm^{-1}). In addition, peaks at 390 nm (ε = 5547 M^{-1} cm^{-1}) and 337 nm (ε = 9347 M^{-1} cm^{-1}) along with a sharp peak at 305 nm (ε = 14062 M^{-1} cm^{-1}) are observed (Fig. 3). To interpret the electronic spectrum of the complex singlet-singlet vertical electronic excitations were calculated by TDDFT/CPCM method in acetonitrile. The low energy broad peak at 446 nm corresponds to HOMO → LUMO transition ($\lambda_{calc.}$ = 477 nm, Osc. Strength (f) = 0.035) having mixed metal to ligand charge transfer (MLCT) and intra-ligand charge transfer (ILCT) character. The band at 390 nm corresponds to HOMO-2 → LUMO transition ($\lambda_{calc.}$ = 403 nm, Osc. Strength (f) = 0.047) with mixed MLCT and XLCT (halogen to ligand charge transfer) character, while the bands at 337 nm and 305 nm have ILCT character (Table 4).

3.5. Electrochemistry

The electrochemical behavior of the complex was investigated by cyclic voltammetry (CV) in presence of Bu_4NPF_6 in acetonitrile at scan rate 50 mV S^{-1}. Cyclic voltammogram exhibits one quasireversible oxidation couple at 1.12 V (ΔE = 96 mV) along with one reversible reduction couple at -0.89 V (ΔE = 74 mV) and an irreversible cathodic reduction peak with E_{pc}, -1.75 V, positive and negative to reference electrode (Ag/AgCl) respectively in the potential range 2.0 to –2.0 V (Fig. 4). The oxidation process may be assigned as Ru(II) to Ru(III) oxidation or the oxidation of redox active ONS ligand as the HOMO has 36% $d\pi$(Ru) and 50% π(L) character. The reversible reduction couple at -0.89 V corresponds to $L/L^{\bullet-}$ reduction as the LUMO has 94% π^*(L) character with major contribution of π^*(N=N) orbital (42%). The cathodic peak at -1.75 V corresponds to further reduction of $L^{\bullet-}$ to L^{2-} in the complex.

3.6. Catalytic transfer hydrogenation

The transfer hydrogenation is an important and efficient reaction in organic synthesis. Many ruthenium(II) complexes were used as effective catalysts for transfer hydrogenation reactions, which encourage us to use our synthesized complex for this purpose.

Initially to determine the catalytic efficiency of complex **1** for the conversion of acetophenone to 1-phenylethanol as a model reaction using ^{i}PrOH as the solvent was carried out in presence of different bases. The conversion was found to be effective in presence of KOH in comparison to Na_2CO_3, CH_3COONa or KO^{t}Bu. Again, to understand the catalytic efficiency of the complex **1**, different catalyst:substrate (C:S) ratios were tested in the transfer hydrogenation of acetophenone in *i*-PrOH/KOH and the results are given in Table 5. It is found that the conversion is excellent in C:S ratio of 1:200. With the variation of C:S ratio to 1:400, 1:600, 1:800, 1:1000 or 1:1200, the reaction still proceeds but a sharp decrease in rate of conversion is observed for C:S ratio 1:600 to 1:1200. The conversion is excellent with appreciable turnover number (TON) when the C:S ratio is 1:400 and hence this C:S ratio is the best choice for catalytic transfer hydrogenation reactions for complex **1**. A series of ketones were screened in transfer hydrogenation reaction using the optimum condition, C:S ratio of 1:400 and KOH as base. The results are summarized in Table 6. The maximum conversion was observed for *p*-nitroacetophenone (98.3%). The conversions of other acetophenones were found to be in the range 88-98%. The results are comparable to the other reported ruthenium(II) complexes [58-61].

4. Conclusion

Herein we have successfully synthesized and characterized ruthenium(II) mixed ligand complex, [Ru(dppp)(L)Cl] (**1**) (where, dppp = bis(diphenylphosphino)propane). The distorted octahedral geometry is confirmed by X-ray diffraction method. Cyclic voltammetric study supports the participation of both Ru(II) and redox active ONS ligand in the redox processes. The efficiency of the complex towards transfer hydrogenation reaction of ketones is studied and 90-98% conversions are observed. Theoretical results obtained by DFT/B3LYP method well interpreted the electronic structure and redox properties of the complex.

Acknowledgement

Financial support received from the Department of Science and Technology, New Delhi, India is gratefully acknowledged. S. Biswas and P. Roy thankful to UGC, New Delhi, India for fellowships.

Supplementary materials

Crystallographic data for the structure **1** was deposited with the Cambridge Crystallographic Data center with the CCDC No. 1056208. Copies of this information may be obtained free of charge from the Director, CCDC, 12 Union Road, Cambridge CB2 1EZ, UK (e-mail: deposit@ccdc.cam.ac.uk or www:htpp://www.ccdc.cam.ac.uk).

References

[1] J.K. Whitesell, Chem. Rev. 89 (1989) 1581-1590.

[2] P.L. Floch, Coord. Chem. Rev. 250 (2006) 627-681.

[3] C.A. Tolman, Chem. Rev. 77 (1977) 313-348.

[4] J.M. Brown, Chem. Soc. Rev. 22 (1993) 25-41.

[5] M. Sunjuk, M. Al-Noaimi, G. Abu Sheikha, E. Lindner, B. El-Eswed, K. Sweidan, Polyhedron 28 (2009) 1393-1398.

[6] J.A. Cabeza, J.M. Fernandez-Colinas, A. Llamazares, V. Riera, Organometallics 12 (1993) 4141-4144.

[7] M.N. Golovin, Organometallics 4 (1985) 1981-1991.

[8] D. Wang, D. Astruc, Chem. Rev. 115 (2015) 6621-6686.

[9] M. Yoshimura, S. Tanaka, M. Kitamura, Tetrahedron Lett. 55 (2014) 3635-3640.

[10] J. Ito, H. Nishiyama, Tetrahedron Lett. 55 (2014) 3133-3146.

[11] R. Malacea, R. Poli, E. Manoury, Coord. Chem. Rev. 254 (2010) 729-752.

[12] T. Ikariya, A.J. Blacker, Acc. Chem. Res. 40 (2007) 1300-1308.

[13] J.S.M. Samec, J.E. Bäckvall, P.G. Andersson, P. Brandt, Chem. Soc. Rev. 35 (2006) 237-248.

[14] J. Magano, J.R. Dunetz, Org. Process Res. Dev. 16 (2012) 1156-1184.

[15] T. Wang, X.Q. Hao, X.X. Zhang, J.F. Gong, M.P. Song, Dalton Trans. 40 (2011) 8964-8976.

[16] E. de Julián, J. Díez, E. Lastra, M.P. Gamasa, J. Mol. Catal. A Chem. 394 (2014) 295-302.

[17] M. Aydemir, N. Meric, C. Kayan, F. Ok, A. Baysal, Inorganica Chim. Acta 398 (2013) 1-10.

[18] G. Chelucci, S. Baldino, W. Baratta, Coord. Chem. Rev. 300 (2015) 29-85.

[19] S. Karabuga, S. Bars, I. Karakaya, S. Gumus, Tetrahedron Lett. 56 (2015) 101-104.

[20] K. Abdur-Rashid, S.E. Clapham, A. Hadzovic, J.N. Harvey, A.J. Lough, R.H. Morris, J. Am. Chem. Soc. 124 (2002) 15104-15118.

[21] H. Doucet, T. Ohkuma, K. Murata, T. Yokozawa, M. Kozawa, E. Katayama, A.F. England, T. Ikariya, R. Noyori, Angew. Chem., Int. Ed. 37 (1998) 1703-1707.

[22] R. Noyori, T. Ohkuma, Angew. Chem., Int. Ed. 40 (2001) 40-73.

[23] K. Abdur-Rashid, M. Faatz, A.J. Lough, R.H. Morris, J. Am. Chem. Soc. 123 (2001) 7473-7474.

[24] R. Noyori, M. Yamakawa, S. Hashiguchi, J. Org. Chem. 66 (2001) 7931-7944.

[25] C. Nachtigal, S. Al Gharabli, K. Eichele, E. Lindner, H.A. Mayer, Organometallics 21 (2002) 105-112.

[26] E. Lindner, A. Ghanem, I. Warad, K. Eichele, H.A. Mayer, V. Schurig, Tetrahedron: Asymmetry 14 (2003) 1045-1053.

[27] M. S. Jana, A. K. Pramanik, S. Kundu, D. Sarkar, S. Jana, T. K. Mondal, Inorg. Chim. Acta 394 (2013) 583-590.

[28] R. Sarkar, K. K. Rajak, J. Organomet. Chem. 779 (2015) 1-13.

[29] A. K. Pramanik, T. K. Mondal, Inorg. Chim. Acta 411 (2014) 106-112.

[30] S. Jana, M.S. Jana, D. Sarkar, M.K. Paira, T.K. Mondal, J. Mol. Struc. 1054-1055 (2013) 83-88.

[31] J.L. Pratihar, S. Bhaduri, P. Pattanayak, D. Patra, S. Chattopadhyay, J. Organomet. Chem. 694 (2009) 3401-3408.

[32] W. Chen, F.N. Rein, R.C. Rocha, Angew. Chem. Int. Ed. 48 (2009) 9672-9675.

[33] R. Ramachandran, G. Prakash, M. Nirmala, P. Viswanathamurthi, J.G. Malecki, J. Organomet. Chem. 791 (2015) 130-140.

[34] M.M. Tamizh, K. Mereiter, K. Kirchner, R. Karvembu, J. Organomet. Chem. 700 (2012) 194-201.

[35] S.K. Sarkar, M.S. Jana, T.K. Mondal, C. Sinha, Appl. Organometal. Chem. 28 (2014) 641-651.

[36] S. Biswas, P. Roy, D. Sarkar, T.K. Mondal, Indian J. Chem. 55A (2016) 929-937.

[37] S. Kundu, D. Sarkar, S. Biswas, S. Jana, T.K. Mondal, J. Indian Chem. Soc. 92 (2015) 1847-1853.

[38] S. Jana, M.S. Jana, S. Biswas, C. Sinha, T.K. Mondal, J. Mol. Struc. 1065-1066 (2014) 52-60.

[39] M.K. Paira, T.K. Mondal, E. López-Torres, J. Ribas, C. Sinha, Polyhedron 29 (2010) 3147-3156.

[40] Bruker-AXS Bruker-AXS, Madison, Wisconsin U.S.A., 2009.

[41] SHELXS97: G.M. Sheldrick, *SHELX97,* Programs for Crystal Structure Analysis (release 97-2); University of Göttingen: Göttingen, Germany (1997).

[42] A.D. Becke, J. Chem. Phys. 98 (1993) 5648-5652.

[43] C. Lee, W. Yang, R.G. Parr, Phys. Rev. B 37 (1988) 785-789.

[44] P.J. Hay, W.R. Wadt, J. Chem. Phys. 82 (1985) 270-283.

[45] W.R. Wadt, P.J. Hay, J. Chem. Phys. 82 (1985) 284-298.

[46] P.J. Hay, W.R. Wadt, J. Chem. Phys. 82 (1985) 299-310.

[47] R. Bauernschmitt, R. Ahlrichs, Chem. Phys. Lett. 256 (1996) 454-464.

[48] R.E. Stratmann, G.E. Scuseria, M.J. Frisch, J. Chem. Phys. 109 (1998) 8218-8224.

[49] M.E. Casida, C. Jamorski, K.C. Casida, D.R. Salahub, J. Chem. Phys. 108 (1998) 4439-4449.

[50] V. Barone, M. Cossi, J. Phys. Chem. A 102 (1998) 1995-2001.

[51] M. Cossi, V. Barone, J. Chem. Phys. 115 (2001) 4708-4717.

[52] M. Cossi, N. Rega, G. Scalmani, V. Barone, J. Comput. Chem. 24 (2003) 669-681.

[53] Gaussian 09, Revision D.01, M. J. Frisch, G. W. Trucks, H. B. Schlegel, G. E. Scuseria, M. A. Robb, J. R. Cheeseman, G. Scalmani, V. Barone, B. Mennucci, G. A. Petersson, H. Nakatsuji, M. Caricato, X. Li, H. P. Hratchian, A. F. Izmaylov, J. Bloino, G. Zheng, J. L. Sonnenberg, M. Hada, M. Ehara, K. Toyota, R. Fukuda, J. Hasegawa, M. Ishida, T. Nakajima, Y. Honda, O. Kitao, H. Nakai, T. Vreven, J. A. Montgomery, Jr., J. E. Peralta, F. Ogliaro, M. Bearpark, J. J. Heyd, E. Brothers, K. N. Kudin, V. N. Staroverov, R. Kobayashi, J. Normand, K. Raghavachari, A. Rendell, J. C. Burant, S. S. Iyengar, J. Tomasi, M. Cossi, N. Rega, J. M. Millam, M. Klene, J. E. Knox, J. B. Cross, V. Bakken, C. Adamo, J. Jaramillo, R. Gomperts, R. E. Stratmann, O. Yazyev, A. J. Austin, R. Cammi, C. Pomelli, J.

W. Ochterski, R. L. Martin, K. Morokuma, V. G. Zakrzewski, G. A. Voth, P. Salvador, J. J. Dannenberg, S. Dapprich, A. D. Daniels, Ö. Farkas, J. B. Foresman, J. V. Ortiz, J. Cioslowski, and D. J. Fox, Gaussian, Inc., Wallingford CT (2009).

[54] N. M. O'Boyle, A. L. Tenderholt, K. M. Langner, J. Comput. Chem. 29 (2008) 839-845.

[55] P. Roy, A. Sau, Mondal, A.K. Pramanik, T.K. Mondal, J. Organomet. Chem. 828 (2017) 1-9.

[56] M. Al-Noaimi, M.I. El-Barghouthi, O.S. Abdel-Rahman, S.F. Haddad, A. Rawashdeh, Polyhedron 30 (2011) 1884-1890.

[57] M. Al-Noaimi, M. Sunjuk, M. El-khateeb, S.F. Haddad, A. Haniyeh, M. AlDamen, Polyhedron 42 (2012) 66-73.

[58] P.K. Suganthy, R. N. Prabhu, V.S. Sridevi, Polyhedron 88 (2015) 57-62.

[59] H.S. Calik, E. Ispir, S. Karabuga, M. Aslantas, J. Organomet. Chem. 801 (2016) 122-129.

[60] L. Zeng, F. Wu, Y.-Y. Li, Z.-R. Dong, J.-X. Gao, J. Organomet. Chem. 762 (2014) 34-39.

[61] A. Kanchanadevi, R. Ramesh, N. Bhuvanesh, J. Organomet. Chem. 788 (2015) 49-57.

Table 1. Crystallographic data and refinement parameters for [Ru(dppp)(L)Cl] (**1**)

Empirical formula	$C_{39}H_{39}ClN_2O_2P_2RuS$
Formula weight	798.24
Crystal system	*Monoclinic*
Space group	*P21/n*
a / Å	13.1224(5)
b / Å	8.4006(3)
c / Å	33.1797(12)
β (°)	100.255(2)
V / Å^3	3599.2(2)
Z	4
ρ_{calcd} / g cm^{-3}	1.473
μ / mm^{-1}	0.694
T / K	293(2)
hkl range	-15 to16, -10 to 10, -40 to 40
F(000)	1640
θ range (°)	1.59 to 25.76
Reflns collected	51552
Unique reflns (R_{int})	6846
Observed data ($I>2\sigma(I)$)	4490
Data/restraints/parameters	6846 / 0 / 433
R1, wR2 ($I>2\sigma(I)$)	0.0523, 0.0872
GOF	0.987
Largest diff. peak/hole / e Å^{-3}	0.826/ -0.795

Table 2. X-ray and calculated bond distances (Å) and angles (°) of **1**

Bond (Å)	X-ray	Calc.
Ru1-Cl1	2.4680(10)	2.494
Ru1-S1	2.3031(10)	2.367
Ru1-P1	2.2802(11)	2.351
Ru1-P2	2.3602(11)	2.420
Ru1-O1	2.052(2)	2.078
Ru1-N2	2.044(3)	2.077
O1-C1	1.267(4)	1.264
O2-C4	1.218(4)	1.227
N1-N2	1.288(4)	1.280
Angles (°)		
N2-Ru1-O1	87.62(11)	87.70
N2-Ru1-P1	90.46(9)	92.15
N2-Ru1-P2	176.80(9)	176.36
N2-Ru1-S1	84.33(9)	84.11
N2-Ru1-Cl1	81.83(9)	82.11
O1-Ru1-P1	93.29(7)	92.36
O1-Ru1-P2	90.19(8)	90.91
O1-Ru1-S1	171.90(8)	171.66
O1-Ru1-Cl1	83.95(7)	83.99
P1-Ru1-S1	87.70(4)	89.55
P1-Ru1-P2	92.00(4)	91.25
P1-Ru1-Cl1	171.90(4)	173.31
P2-Ru1-S1	97.81(4)	97.15
P2-Ru1-Cl1	95.62(4)	94.34
S1-Ru1-Cl1	93.98(4)	93.26

Table 3. Energy and composition of selected molecular orbitals of **1**

MOs	Energy (eV)	% of composition			
		Ru	L	Cl	dppp
LUMO+5	-0.41	11	28	01	60
LUMO+4	-0.45	02	26	0	72
LUMO+3	-0.61	03	02	0	95
LUMO+2	-0.72	01	05	0	94
LUMO+1	-0.88	22	15	05	58
LUMO	-1.63	03	94	0	03
HOMO	-5.08	36	50	10	04
HOMO-1	-5.43	47	24	23	06
HOMO-2	-5.45	33	21	39	07
HOMO-3	-5.73	29	41	24	06
HOMO-4	-6.00	18	78	03	01
HOMO-5	-6.32	12	33	32	28
HOMO-6	-6.48	20	18	32	30
HOMO-7	-6.56	11	63	17	09
HOMO-8	-6.59	07	21	11	61
HOMO-9	-6.74	04	06	02	88
HOMO-10	-6.80	05	09	04	82

Table 4. Selected vertical electronic transitions calculated by TDDFT/CPCM method and experimental λ_{max} (nm)

$E_{excitation}$ (eV)	$\lambda_{excitation}$ (nm)	Osc. Strength (f)	Key transitions	Character	$\lambda_{expt.}$ (nm) (ε, $M^{-1}cm^{-1}$)
2.6013	476.6	0.0353	(85%) HOMO → LUMO	$\pi(L)/d\pi(Ru) \rightarrow \pi^{*}(L)$	466 (3907)
2.7430	452.00	0.0140	(75%) HOMO-1 → LUMO	$\pi(L)/d\pi(Ru) \rightarrow \pi^{*}(L)$	
3.0790	402.7	0.0476	(78%) HOMO-2 → LUMO	$p\pi(Cl)/d\pi(Ru) \rightarrow \pi^{*}(L)$	390 (5547)
3.5409	350.1	0.1163	(69%) HOMO-4 → LUMO	$\pi(L) \rightarrow \pi^{*}(L)$	337 (9347)
4.1984	295.3	0.0401	(67%) HOMO - 7 → LUMO	$\pi(L) \rightarrow \pi^{*}(L)$	305 (14062)

Table 5. Effect of S:C ratio on the transfer hydrogenation of acetophenone[a]

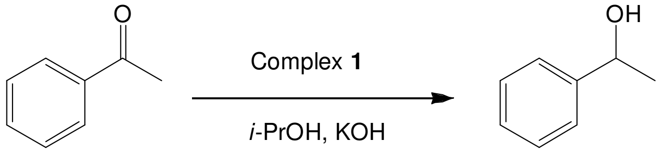

Entry	S:C ratio	Conversion[b] (%)	TON[c]
1	1:200	96.4	193
2	1:400	95.2	381
3	1:600	88.4	530
4	1:800	75.1	601
5	1:1000	59.5	595
6	1:1200	35.2	422

[a] Reaction condition: acetophenone (2 mmol), complex **1** (10-0.8 μmol), catalyst:KOH 1:4 in *i*-PrOH (10 mL) at 80 °C for 5 h; [b] Conversion was determined by GC analysis; [c] Turnover number (TON) = mole of product/mol of catalyst.

Table 6. Catalytic transfer hydrogenation of ketones using complex **1**[a]

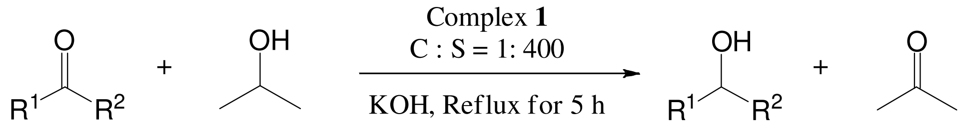

Entry	Ketones	Alcohols	Conv. (%)[b]	TON[c]	Entry	Ketones	Alcohols	Conv. (%)[b]	TON[c]
1	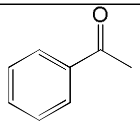	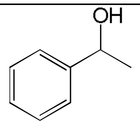	95.2	381	7	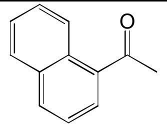	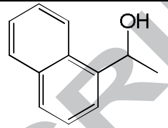	89.6	358
2	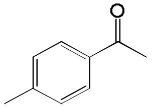	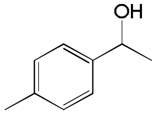	96.6	386	8	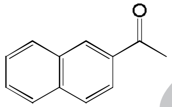	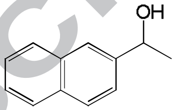	87.9	352
3	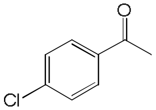	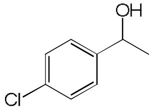	97.2	389	9	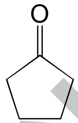	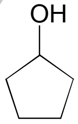	95.7	383
4	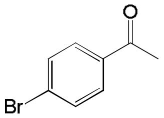	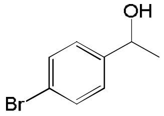	97.4	390	10	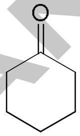	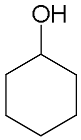	94.3	377
5	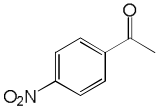	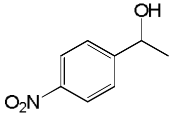	98.3	393	11	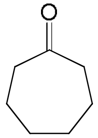	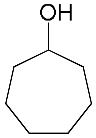	91.2	365
6	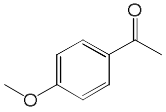	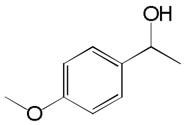	98.1	392	12	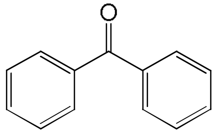	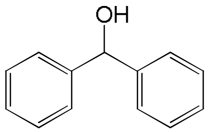	87.6	350

[a] Experimental condition: reactions were carried out at 80 °C, ketone (1.0 mmol), complex **1** (0.25 mol%), KOH (0.1 mmol), *i*-PrOH (10 mL); [b] Conversion was determined by GC analysis; [c] Turnover number (TON) = mole of product/mol of catalyst.

Figure captions

Fig. 1. ORTEP plot with 35% ellipsoidal probability of [Ru(dppp)(L)Cl] (**1**)

Fig. 2. Contour plots of selected molecular orbitals of **1**

Fig. 3. UV-Vis spectrum of **1** in acetonitrile

Fig. 4. Cyclic voltammogram of **1** in acetonitrile

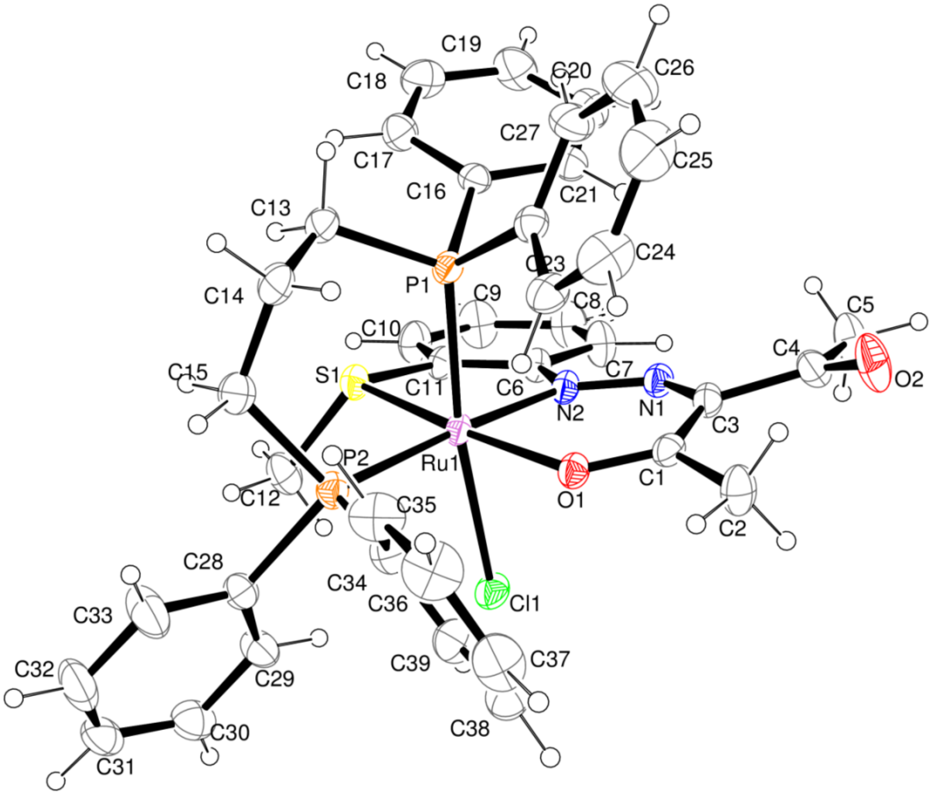
C19
C18
C20
C26
C27
C25
C17
C16
C21
C13
C24
C23
P1
C9
C14
C8
C10
C5
C4
C15
S1
C11
C6
C7
N1
O2
N2
C3
P2
Ru1
C1
C12
C35
O1
C2
C28
C34
C36
Cl1
C33
C37
C39
C32
C29
C38
C30
C31

Fig. 1

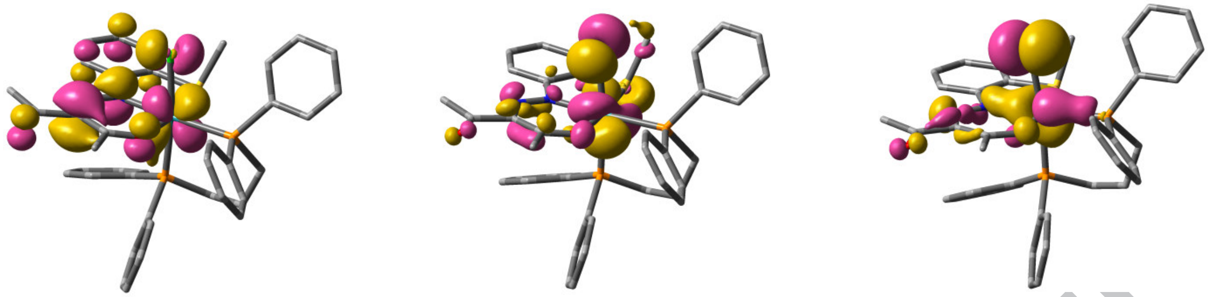

HOMO HOMO-1 HOMO-2

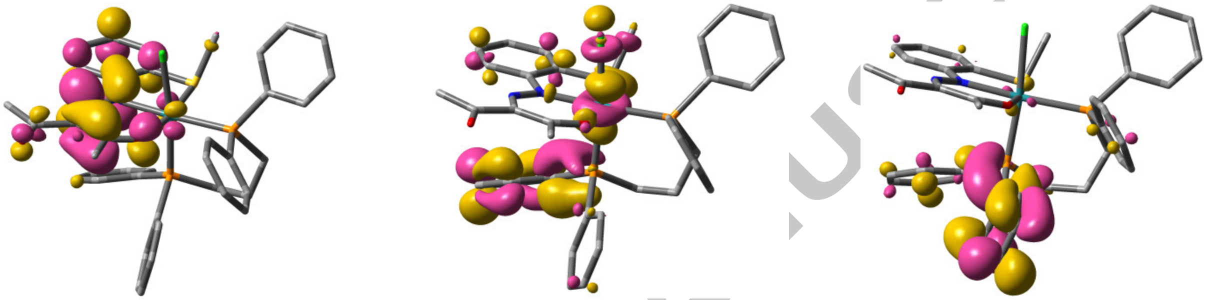

LUMO LUMO+1 LUMO+2

Fig. 2

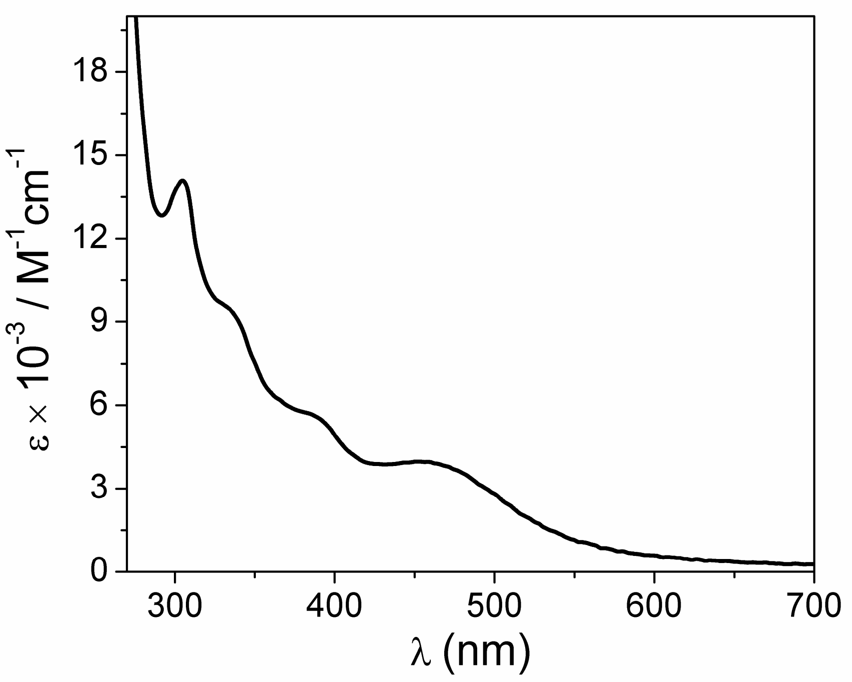

Fig. 3

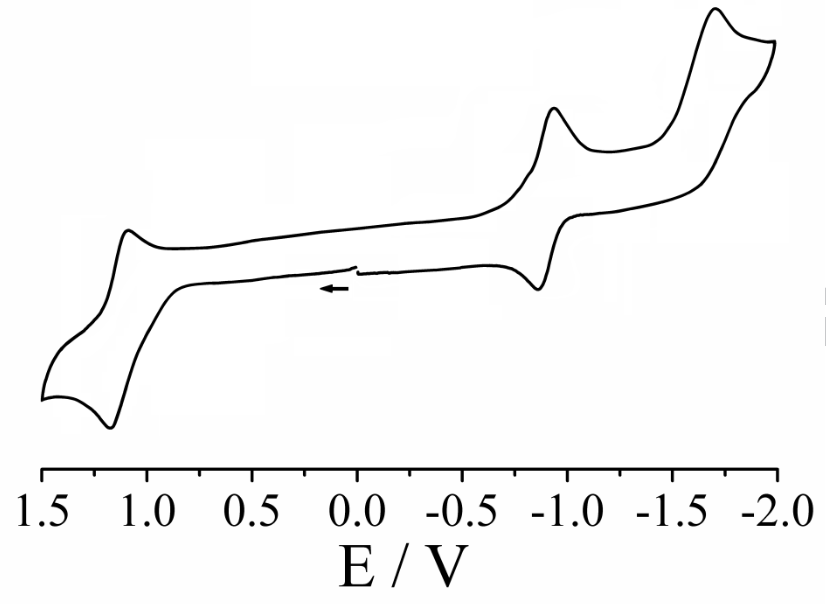

Fig. 4

GRAPHICAL ABSTRACT

Synthesis and characterization of a ruthenium complex with bis(diphenylphosphino)propane and thioether containing ONS donor ligand: Application in transfer hydrogenation of ketones

Sujan Biswas, Deblina Sarkar, Puspendu Roy and Tapan Kumar Mondal

Ruthenium mixed ligand complex, [Ru(dppp)(L)Cl] (**1**) (where, dppp = bis(diphenylphosphino)propane) has been synthesized by the reaction of $RuCl_3.3H_2O$, dppp and HL under refluxing condition (HL = 3-(2-(2-(methylthio)phenyl)hydrazono)pentane-2,4-dione). X-ray structure exhibits distorted octahedral geometry around ruthenium. Cyclic voltammetric study supports the participation of both Ru(II) and redox active ONS ligand in the redox processes. The complex efficiently catalyzed the transfer hydrogenation of ketones in *i*-PrOH.

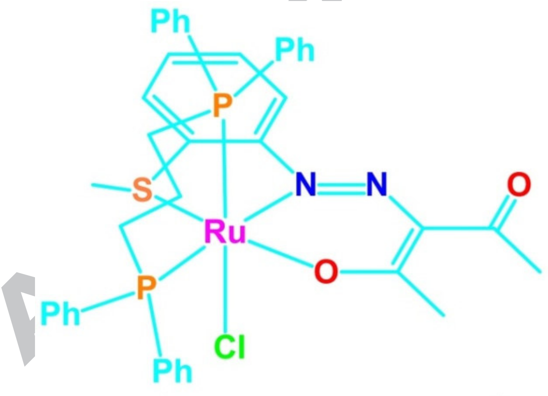

[Ru(dppp)(L)Cl] (1)

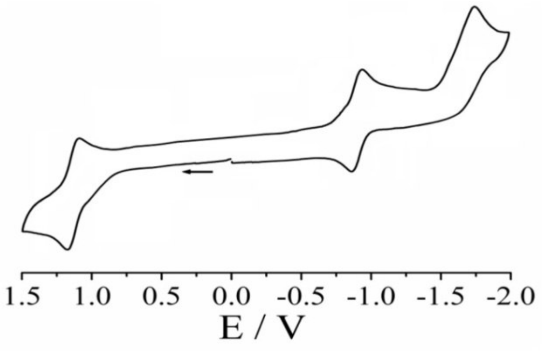

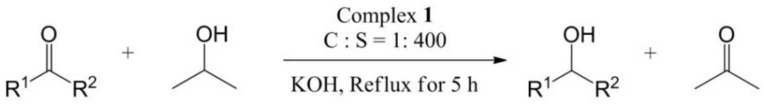

PICTORIAL ABSTRACT

Synthesis and characterization of a ruthenium complex with bis(diphenylphosphino)propane and thioether containing ONS donor ligand: Application in transfer hydrogenation of ketones

Sujan Biswas, Deblina Sarkar, Puspendu Roy and Tapan Kumar Mondal

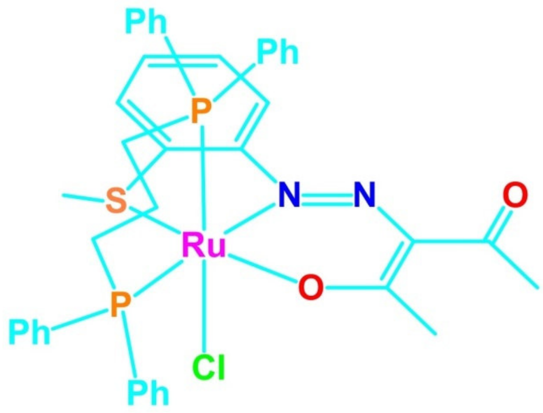

[Ru(dppp)(L)Cl] (1)